AJNR

MR Imaging and Clinical Characteristics of Diffuse Glioneuronal Tumor with Oligodendroglioma-like Features and Nuclear Clusters

M. Benesch, T. Perwein, G. Apfaltrer, T. Langer, A. Neumann, I.B. Brecht, M.U. Schuhmann, H. Cario, M.C. Frühwald, K. Vollert, M. van Buiren, M.Y. Deng, A. Seitz, C. Haberler, M. Mynarek, C. Kramm, F. Sahm, P.A. Robe, J.W. Dankbaar, K.V. Hoff, M. Warmuth-Metz and B. Bison

AJNR Am J Neuroradiol published online 22 September 2022
http://www.ajnr.org/content/early/2022/09/22/ajnr.A7647

Published September 22, 2022 as 10.3174/ajnr.A7647

MR Imaging and Clinical Characteristics of Diffuse Glioneuronal Tumor with Oligodendroglioma-like Features and Nuclear Clusters

M. Benesch, T. Perwein, G. Apfaltrer, T. Langer, A. Neumann, I.B. Brecht, M.U. Schuhmann, H. Cario, M.C. Frühwald, K. Vollert, M. van Buiren, M.Y. Deng, A. Seitz, C. Haberler, M. Mynarek, C. Kramm, F. Sahm, P.A. Robe, J.W. Dankbaar, K.V. Hoff, M. Warmuth-Metz, and B. Bison

ABSTRACT

BACKGROUND AND PURPOSE: Diffuse glioneuronal tumor with oligodendroglioma-like features and nuclear clusters (DGONC) is a new, molecularly defined glioneuronal CNS tumor type. The objective of the present study was to describe MR imaging and clinical characteristics of patients with DGONC.

MATERIALS AND METHODS: Preoperative MR images of 9 patients with DGONC (median age at diagnosis, 9.9 years; range, 4.2–21.8 years) were reviewed.

RESULTS: All tumors were located superficially in the frontal/temporal lobes and sharply delineated, displaying little mass effect. Near the circle of Willis, the tumors encompassed the arteries. All except one demonstrated characteristics of low-to-intermediate aggressiveness with high-to-intermediate T2WI and ADC signals and bone remodeling. Most tumors ($n = 7$) showed a homogeneous ground-glass aspect on T2-weighted and FLAIR images. On the basis of the original histopathologic diagnosis, 6 patients received postsurgical chemo-/radiotherapy, 2 were irradiated after surgery, and 1 patient underwent tumor resection only. At a median follow-up of 61 months (range, 10–154 months), 6 patients were alive in a first complete remission and 2 with stable disease 10 and 21 months after diagnosis. The only patient with progressive disease was lost to follow-up. Five-year overall and event-free survival was 100% and 86±13%, respectively.

CONCLUSIONS: This case series presents radiomorphologic characteristics highly predictive of DGONC that contrast with the typical aspects of the original histopathologic diagnoses. This presentation underlines the definition of DGONC as a separate entity, from a clinical perspective. Complete resection may be favorable for long-term disease control in patients with DGONC. The efficacy of nonsurgical treatment modalities should be evaluated in larger series.

ABBREVIATIONS: DNET = dysembryoplastic neuroepithelial tumor; HIT = Brain Tumor Network; DGONC = diffuse glioneuronal tumor with oligodendroglioma-like features and nuclear clusters; PNET = primitive neuroectodermal tumor

For decades, the pathologic diagnosis and classification of tumors of the CNS have been almost exclusively based on histomorphologic features.[1] Recently, molecular profiling has revolutionized our understanding of CNS tumors, leading to the definition of new entities and improved risk stratification.[2-5] Further effort has been made to correlate newly defined molecular subgroups with clinical features and neuroradiologic findings.[6-13]

Received January 25, 2022; accepted after revision June 28.

From the Division of Pediatric Hematology and Oncology (M.B., T.P.), Department of Pediatrics and Adolescent Medicine, and Division of Pediatric Radiology (G.A.), Department of Radiology, Medical University Graz, Graz, Austria; Departments of Pediatrics (T.L.) and Neuroradiology (A.N.), University Medical Center Schleswig-Holstein, Campus Lübeck, Lübeck, Germany; Pediatric Hematology and Oncology (I.B.B.), Children's Hospital, and Division of Pediatric Neurosurgery (M.U.S.), Department of Neurosurgery, Eberhard-Karls University Tübingen, Tübingen, Germany; Department of Pediatrics and Adolescent Medicine (H.C.), Ulm University Medical Center, Ulm, Germany; Swabian Children's Cancer Center (M.C.F.), Pediatric and Adolescent Medicine and Departments of Diagnostic and Interventional Radiology and Neuroradiology (K.V., B.B.), University Medical Center Augsburg, Augsburg, Germany; Department of Pediatric Hematology and Oncology (M.v.B.), Center for Pediatrics, Medical Center-University of Freiburg, Freiburg, Germany; Hopp Children's Cancer Center Heidelberg (M.Y.D., F.S.), German Cancer Research Center and Department of Neuroradiology (A.S.), Department of Neuropathology (F.S.), Institute of Pathology, and Clinical Cooperation Unit Neuropathology (F.S.), German Cancer Consortium, German Cancer Research Center, Heidelberg University Hospital, Heidelberg, Germany; Division of Neuropathology and Neurochemistry (C.H.), Department of Neurology, Medical University of Vienna, Vienna, Austria; Department of Pediatric Hematology and Oncology (M.M.) and Mildred Scheel Cancer Career Center (M.M.), University Medical Center Hamburg-Eppendorf, Hamburg, Germany; Division of Pediatric Hematology and Oncology (C.K.), University Medical Center Göttingen, Göttingen, Germany; Department of Neurology and Neurosurgery (P.A.R.) and Department of Radiology (J.W.D.), University Medical Center Utrecht, Utrecht, the Netherlands; Department of Pediatric Oncology and Hematology (K.V.H.), Charité–Universitätsmedizin Berlin, corporate member of Freie Universität Berlin, Humboldt-Universität zu Berlin, and Berlin Institute of Health, Berlin, Germany; and Institute of Diagnostic and Interventional Neuroradiology (M.W.-M.), University Hospital Würzburg, Würzburg, Germany.

Since the late 1980s, the Brain Tumor Network (HIT) of the Society of Pediatric Oncology and Hematology (GPOH, Gesellschaft für Pädiatrische Onkologie und Hämatologie) in Germany, Austria and Switzerland has run a series of disease-specific treatment optimization and observational studies for children with CNS tumors.

These studies have allowed exploring novel therapeutic options and provide standardized treatment recommendations as well as a system of high-quality reference diagnostics and expert counseling for diagnostics and therapy. Along with neuropathologic reference diagnostics, the central neuroradiologic review at the Neuroradiological Reference Center of the HIT group (Department of Diagnostic and Interventional Neuroradiology, University Hospital, Augsburg, Germany) has become a mandatory practice for all recruited patients. The MR imaging series of the HIT studies have been archived on the Medical Data and Picture Exchange server by the Medical Informatics Group at the University Hospital, Frankfurt, Germany, which enables their rapid access for re-review to address scientific questions. Thus, the objective of performing the present case series was to describe MR imaging and corresponding clinical characteristics of diffuse glioneuronal tumors with oligodendroglioma-like features and nuclear clusters (DGONC), a molecularly defined glioneuronal CNS tumor class that has been described recently and has been included as a provisional tumor type in the 2021 World Health Organization Classification of CNS Tumors.[5,14,15]

MATERIALS AND METHODS

The (retrospective) neuropathologic diagnosis of DGONC was initially made according to the DNA methylation profile and other criteria (nuclear clusters of small-to-medium-sized cells with oligodendroglioma-like morphology, *OLIG2* and synaptophysin expression, and the absence of widespread glial fibrillary acidic protein expression, monosomy 14) as previously described.[5,14] MR images of 9 patients were then retrospectively re-evaluated by an experienced neuroradiologist (B.B.). MR imaging series from 8 patients had been sent for central neuroradiologic review at the time of diagnosis, allowing their inclusion in the respective treatment optimization study or registry. In the ninth patient, the MR imaging was provided by colleagues from the Princess Máxima Center for Pediatric Oncology, Utrecht, Netherlands. In all cases, MR images were obtained at the initial diagnosis.

MR imaging data were generated at local centers with MR imaging scanners from different manufacturers at 1.5T or 3T field strength. In all patients, basic MR imaging data sets of the brain included T2WI, FLAIR, or proton density sequences; T1WI without and with contrast enhancement; as well as DWI with ADC. In 6 patients, additional MRIs of the spine, including T1WI with contrast enhancement of the entire dural sac, were available.

The evaluation was performed according to standardized MR imaging criteria adapted from the routine image evaluation at the Neuroradiological Reference Center, including localization, size (calculated as an approximation of the ellipsoid formula and using the maximum diameters in the 3 standard planes [axial × coronal × sagittal × 0.5 cm^3]), contour, peritumoral edema, mass effect, and contrast enhancement estimated as part of the tumor volume. The intensity of the contrast enhancement was compared with the choroid plexus and quantified in 3 subjective steps of intensity. Clinical characteristics and treatment-related and outcome parameters were retrieved from the respective study centers and retrospectively analyzed without direct personal identification. All patients had received treatment according to their respective original diagnosis before the diagnosis of DGONC was established. Survival curves were calculated with the Kaplan-Meier method using the SPSS Statistics 26 software package (IBM). Informed consent was obtained from the patients or their legal representatives at the time of study inclusion. The present study was approved by the institutional review board of the Ludwig-Maximilians University of Munich, Germany (Publication No. 21–0493). Data were updated as of October 31, 2020.

RESULTS

Imaging Characteristics

Representative MR imaging slices at diagnosis are shown in the Figure (patients 1—9 [P1–P9]). Major MR imaging characteristics are summarized in the Online Supplemental Data. All tumors were localized in the supratentorial region in the frontal or temporal lobes; in 2 cases, the tumor crossed the midline and extended into both frontal lobes (patients 1 and 5). In another patient (patient 2), both the frontal and temporal lobes of the right hemisphere were involved. Eight tumors were located at the basal part of the brain with 4 oriented directly toward the frontobase, with a temporomesial manifestation in 3 cases. Only 1 tumor was located along the convexity (patient 8). Tumors formed a broad basis of the surface of the lobe, involving the cortex and medullary WM in all cases. Displacement of the basal ganglia was common, without definite signs of infiltration of the deep GM. The median initial tumor volume was 35.83 mL (range, 2.28–80.14 mL). Tumors in the temporomesial region and along the convexity were smaller (2.28, 4.86, 10.05, and 5.82 mL) than the remaining tumors.

All tumors were clearly demarcated and sharply contoured, masking the underlying tissue, and had a relatively low mass effect in comparison with their size. This observation was more pronounced in larger tumors (eg, Figure, P1AB, P2AB, P5AB). Edema was absent in 6 and was small (up to 0.7 cm, measured perpendicular to the tumor) in 2 patients (Figure, P4AB, P8AB). A marked edema of 2 cm was found in only 1 patient (Figure, P3A, short gray/white arrows). Of note, imaging characteristics in this patient differed from those of the other patients in several respects. Contrast enhancement was detectable in only 3 patients (patients 3, 8, and 9), all with an intermediate intensity (Figure, P3C, P8C, P9C, Online Supplemental Data); in 2 of these patients, almost the

Martin Benesch and Thomas Perwein share first authorship.

The Neuroradiologic Reference Center of the Brain Tumor Network Consortium, University Würzburg (grant Nos. 2001.05, 2003.09, 2005.07, 2008.07, 2011.02, 2013.21, 2014.15, 2017.07, 2018.02 to M. Warmuth-Metz, B. Bison) were supported by the German Children's Cancer Foundation (Deutsche Kinderkrebsstiftung). M. Benesch and T. Perwein receive support from the Styrian Childhood Cancer Foundation (Steirische Kinderkrebshilfe).

Please address correspondence to Thomas Perwein, MD, Division of Pediatric Hematology and Oncology, Department of Pediatrics and Adolescent Medicine, Medical University of Graz, Auenbruggerplatz 34/2, 8036 Graz, Austria; e-mail: thomas.perwein@medunigraz.at

Indicates article with online supplemental data.

http://dx.doi.org/10.3174/ajnr.A7647

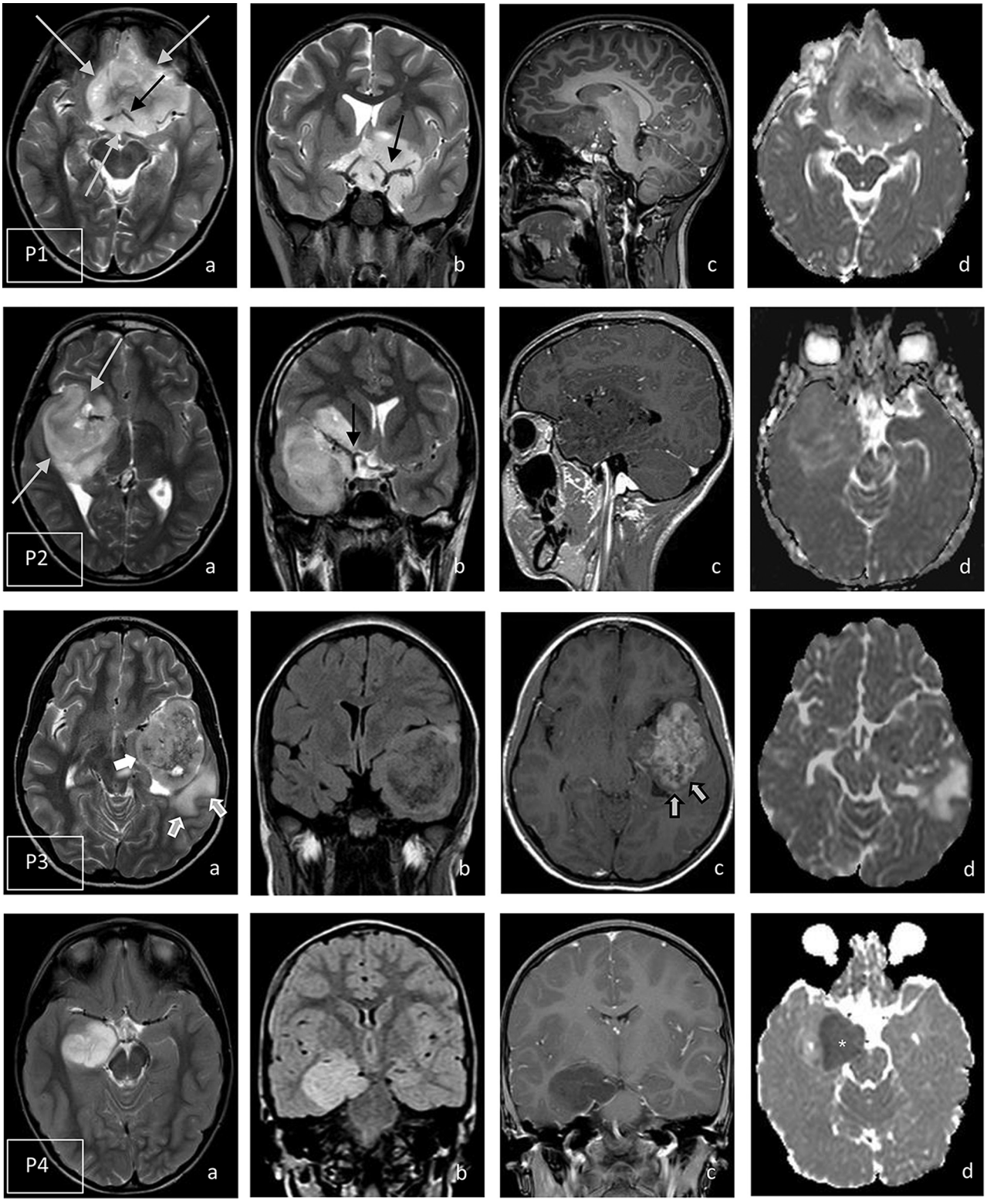

FIGURE. Representative MR imaging slices of all 9 patients (P1–P9). Columns: *A*, Axial T2WI in all MRIs; *B*, Coronal T2WI (P1, P2, P5) and coronal FLAIR (P3, P4, P6, P7, P8, P9); *C*, Contrast-enhanced T1WI, sagittal (P1, P2, P5), axial (P3, P6, P8, P9), or coronal (P4, P7); *D*, axial DWI/ADC in all MRIs. Long gray arrows, centrally decreased T2 signal suggestive of diffuse calcification (P1A, P2A); black arrows, tumor encompassing the circle of Willis and adjacent arteries without compression (P1AB, P2B, P5B, P9B); short gray/white arrows, marked edema (P3A); short white arrows, band-like pattern with intermediate signal on T2WI (P3A, P8A); short gray/black arrows, inhomogeneous band-like CE of the solid tumor part (P3C, P8C); white asterisk, restricted diffusion (P4D); white arrow, patchy pattern of CE affecting <25% of the tumor volume (P9C).

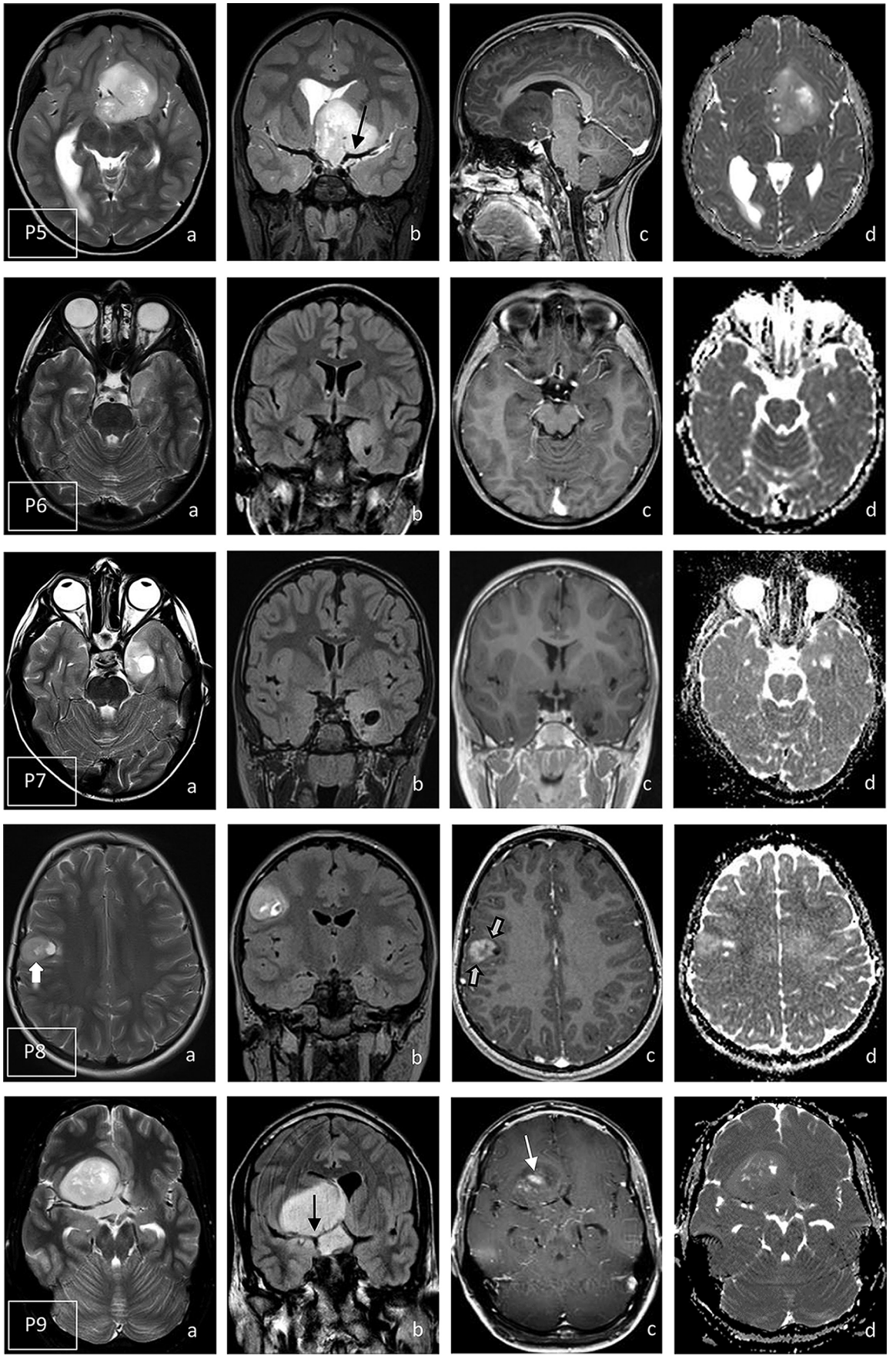

FIGURE. Continued

complete solid part showed an inhomogeneous bandlike enhancement (Figure, P3C and P8C, short gray/black arrows); and in 1 case, the contrast enhancement displayed a patchy pattern that affected <25% of the tumor volume (Figure, P9C, white arrow). The tumor structure was predominantly homogeneous in 7 cases, with a high signal on T2WI in 5 cases (Figure, P1AB, P4AB, P5AB, P7A, P9A) and an intermediate-to-high T2WI signal in 2 cases (Figure, P2AB, P8AB). As a characteristic pattern, we called this homogeneous and sharply contoured aspect "ground-glass-like." In the 2 largest of these structures, the T2 signal was centrally decreased, which was suggestive of diffuse calcification (Figure, P1A, P2A, long gray arrows).

In 2 patients, a bandlike pattern with an intermediate signal on T2WI corresponding to the contrast enhancement was noted (patients 3 and 8; Figure, P3A, P8A, short white arrows). In all except 1 patient, diffusion signals were inhomogeneous, equaling the adjacent brain. Only the patient who had experienced progressive disease before the initiation of treatment had restricted diffusion (patient 4; Figure, P4D, white asterisk). Bone remodeling was present in all cases in which the bone was immediately adjacent to the tumor. Small, not clearly definable defects (either small necroses or cysts or prominent Virchow-Robin spaces) were detected in 8 cases. No relevant necroses or cysts exceeding 10% of tumor volume were found. In the 4 patients with larger frontal or frontotemporal tumors (35.83, 44.46, 64.45, and 80.14 mL), the circle of Willis and adjacent arteries were surrounded by the tumor without any signs of compression visible on the basic MR imaging (Figure, P1B, P2B, P5B, P9B, black arrows). Although blood-sensitive sequences were not available, large areas of hemorrhage and blood-degradation products were not detectable. None of the patients had a leptomeningeal dissemination. Follow-up scans 3.5 months after the initial imaging were available in 1 patient (Online Supplemental Data) and showed a 3-fold tumor volume increase accompanied by a reduction in the T2WI and FLAIR signals. The patient did not receive any treatment between the first and second MR imaging.

Clinical Characteristics

Clinical and treatment characteristics are shown in the Online Supplemental Data. The median age at diagnosis was 9.9 years (range, 4.2–21.8 years) with a female predominance of 2:1. The primary diagnosis was anaplastic glioma in 4 (oligodendroglioma, $n = 3$; oligoastrocytoma, $n = 1$), as well as CNS primitive neuroectodermal tumor (CNS PNET) and CNS neuroblastoma in 2 patients each, respectively. One patient was initially diagnosed with dysembryoplastic neuroepithelial tumor (DNET).

Information about the clinical presentation was available for 6 of 9 patients. Compatible with the tumor site, the most common presenting symptoms were seizures (mainly complex-partial; $n = 5$), while double vision and nausea were reported in 1 patient each.

Treatment Response, Status of Remission, and Survival

Initial complete resection was achieved in 4 patients (Online Supplemental Data). The remaining 5 patients underwent a partial or subtotal resection. In one of these, a complete surgical remission was achieved by a second surgery. Postoperative nonsurgical treatment was guided by the primary histopathologic diagnosis. Only 1 patient (patient 6 with mesial temporal DNET) was treated by surgery (complete resection) alone. All patients with the primary diagnosis of anaplastic glioma ($n = 4$) underwent local irradiation; in 3 of these, temozolomide was administered with concomitant radiation therapy, followed by temozolomide maintenance therapy for 12–18 months. In 1 patient (patient 4), a watch-and-wait strategy was pursued after initial imaging. Three months later, a second MR imaging showed massive progression, leading to surgery and adjuvant therapy. Patients with CNS PNET ($n = 2$) received craniospinal irradiation with tumor boost followed by 8 cycles of maintenance chemotherapy in one of them. One patient with CNS neuroblastoma was also treated with craniospinal irradiation, tumor boost, and maintenance therapy. In the second patient with the initial diagnosis of CNS neuroblastoma, an individualized chemotherapy was administered followed by local irradiation.

With a median follow-up of 61 months (range, 10–154 months), 6 patients were alive in the first continuous complete remission. Two patients were alive with stable residual lesions 10 and 21 months after the initial diagnosis, respectively. The only progression occurred in 1 patient (patient 2) who developed a single metastatic lesion in the right posterior horn of the lateral ventricle following the initial partial resection and local irradiation. After complete re-resection, she received various chemotherapies and was lost to follow-up with progressive disease. The overall and event-free survival rates at 5 years were 100% and 86±13%, respectively.

DISCUSSION

In recent years, there has been an effort to describe imaging features in histopathologically and molecularly defined CNS tumor entities. Ideally, a pathognomonic spectrum of imaging characteristics would allow the number of potential differential diagnoses to be narrowed down on the basis of the neuroradiologic appearance of a tumor. However, previous reports have shown that in general, imaging characteristics, even within a particular tumor subtype, are quite heterogeneous and overlap with various CNS tumor entities.[9-13] Although special criteria exist in childhood brain tumors, the rarity of most brain tumor subtypes hampers the ability to identify unique imaging features and to conduct a reliable statistical analysis. In addition, the availability of standardized, centrally reviewed MR images is limited and is possible only in the context of clinical trials.

The aim of the present analysis was to describe neuroradiologic features with corresponding clinical characteristics in patients with DGONC, a recently and molecularly defined CNS tumor entity.[5,14] Despite their distinct DNA methylation profile, DGONCs display a spectrum of histologic differentiation that varies from well-differentiated tumors with a low mitotic index to undifferentiated cases with brisk mitotic activity. This variability reflects that of the original diagnosis, which ranged from DNET to anaplastic oligodendroglioma and CNS-PNET/neuroblastoma. Still, 7 of the 9 patients in our series had highly similar radiologic characteristics that were distinct from the features expected on the basis of the original diagnoses. In 2 of these 7 patients with cellular, undifferentiated tumors (original diagnosis of CNS neuroblastoma in patient 1 and CNS PNET in patient 9), this

characteristic aspect was particularly remarkable because such tumors would generally have neuroradiologic signs of high cellularity with a low T2WI signal, at least a partly restricted diffusion, an inhomogeneous bandlike or nodular contrast enhancement, extensive necroses, and hemorrhage.

In our cohort, all tumors were located in the frontal and/or temporal lobes in a superficial position, involving the cortical and subcortical white matter. This observation is in accordance with all cases of DGONC reported to date being supratentorial.[5,14,15] Tumor margins were sharp with little mass effect and hyperintense on T2- and FLAIR-weighted sequences, as also described by Pickles et al.[15] Most tumors showed a characteristic homogeneous ground-glass-like aspect on the T2WI and FLAIR images. They displayed characteristics of low-grade tumors without restricted diffusion, the adjacent arteries were surrounded by the tumor without signs of compression, and all tumors near the bone demonstrated bone remodeling, suggesting a clinical behavior similar to that of low-grade glioneuronal tumors, as originally proposed by Deng et al.[14]

Contrast enhancement was seen in only 3 patients, all with an intermediate intensity. One of these patients had the characteristic appearance with a discrete, diffuse contrast enhancement. In 2 of the 9 patients (patients 3 and 8) with the original diagnosis of a World Health Organization grade IV CNS neuroblastoma and CNS PNET, respectively, the radiomorphologic appearance differed from this characteristic aspect, showing a bandlike structure both on the T2WI and contrast-enhanced images. Although the experience in CNS neuroblastoma is still limited, a large size, nodular aspect, severe edema, and contrast enhancement are radiomorphologic features that have been described in these tumors.[16] Former PNET, according to the World Health Organization 2007 classification, would demonstrate aggressive behavior with restricted diffusion, necroses, and hemorrhage. This appearance contrasts with both the regular bandlike aspect of the tumors in these 2 patients, without restricted diffusion or signs of aggressiveness, and the imaging features regarded as characteristic of DGONC in the present study, though PNETs like the DGONCs we describe here appear clearly delineated and mostly without any perifocal edema and little-or-no contrast enhancement.

In 2 patients with relatively small, temporomesial tumors, T2WI signals were elevated but lower compared with the larger tumors. Whether the intensity of the T2WI signal correlates with the tumor size (ie, getting brighter while growing) remains to be explored.

One noteworthy point is that restricted diffusion, usually a sign of high cellularity, was observed in only 1 case (patient 4) in our series and contrasted with the high T2WI signal, typically indicating low cellularity, in this case. This patient developed a 3-fold tumor growth when a watch-and-wait strategy was applied. Further experience is needed to explore whether restricted diffusion in this case is a sign of higher aggressiveness compared with the 8 other cases. Here, the T2WI and FLAIR signals became darker in the follow-up MR imaging examination, though no treatment was administered. Regarding the MR imaging aspect, this finding can be explained by a higher cellularity, which has to be proved in additional patients with DGONC. The histomorphologic diagnosis of DNET is associated with radiomorphologic signs of extremely low cellularity with a very bright signal on T2WI and ADC, as well as a multicystic structure, which also contrasts with the images in our case series. Larger tumors showed a more pronounced inhomogeneity with a centrally lower T2WI signal. On the basis of the diffuse distribution, this phenomenon is highly suggestive of diffuse calcifications.

Most patients in our series had the histopathologic diagnosis of anaplastic oligodendroglioma. Here, we would expect a high level of congruence with DGONC because these are typically well-delineated, cortically-based tumors. However, signs of clumped calcifications, as described by Pickles et al,[15] or hemorrhage were not detectable in our cases. Whether the orientation toward the skull base is another distinct feature suggestive of DGONC needs to be evaluated in future research.

CONCLUSIONS

Most DGONCs (7 of 9) in our series had uniform, characteristic MR imaging features despite a spectrum of histologic differentiation that ranged from well-differentiated to undifferentiated tumors, emphasizing the definition of DGONC as a separate entity from a clinical perspective. These radiomorphologic characteristics clearly differ from the typical MR imaging aspect of the original histomorphologic diagnoses, become increasingly obvious in larger tumors, and are highly predictive of a DGONC. Typical features include the superficial, supratentorial localization with an orientation toward the skull base, as well as involvement of the cortex and white matter, causing only the displacement of the deep gray matter with little-to-no perifocal edema. DGONCs are sharply delineated from the adjacent tissue with little mass effect for their size and display a relatively homogeneous structure that masks the underlying tissue with a bright-to-intermediate T2WI signal, which we call the ground glass-like aspect. In a suprasellar localization, they engulf the arteries of the circle of Willis without any sign of compression or infiltration. Adjacent to bone, they induce bone remodeling.

These aspects resemble low-grade tumors and suggest an intermediate aggressiveness, which is also reflected by the better survival rates compared with those reported for highly malignant CNS tumors. The clinical course ranged from continuous complete remission after total resection to metastatic tumor recurrence with subsequent treatment-refractory progressive disease. Still, no patient died in our series, and disease control was attained in almost 90% of patients following resection with and without adjuvant radio-/chemotherapy. Complete resection may be favorable for long-term disease control in patients with DGONC. Of note, restricted diffusion was found in only 1 patient, though all other criteria of the characteristic DGONC aspect were present. Additional cases have to be analyzed to gain more insight into the relationship between the MR imaging morphology and histologic and molecular diagnoses, as well as into clinical features in patients with DGONC, with the aim of explaining apparent discrepancies in this respect.

Disclosure forms provided by the authors are available with the full text and PDF of this article at www.ajnr.org.

REFERENCES

1. Scheithauer BW. **Development of the WHO classification of tumors of the central nervous system: a historical perspective.** *Brain Pathol* 2009;19:551–64 CrossRef Medline

2. Capper D, Jones DT, Sill M, et al. **DNA methylation-based classification of central nervous system tumours.** *Nature* 2018;555:469–74 CrossRef Medline
3. Sturm D, Orr BA, Toprak UH, et al. **New brain tumor entities emerge from molecular classification of CNS-PNETs.** *Cell* 2016;164:1060–72 CrossRef Medline
4. Louis DN, Perry A, Reifenberger G, et al. **The 2016 World Health Organization classification of tumors of the central nervous system: a summary.** *Acta Neuropathol* 2016;131:803–20 CrossRef Medline
5. Louis DN, Perry A, Wesseling P, et al. **The 2021 WHO Classification of Tumors of the Central Nervous System: a summary.** *Neuro Oncol* 2021;23:1231–51 CrossRef
6. Pajtler KW, Mack SC, Ramaswamy V, et al. **The current consensus on the clinical management of intracranial ependymoma and its distinct molecular variants.** *Acta Neuropathol* 2017;133:5–12 CrossRef Medline
7. Guerreiro Stucklin AS, Ramaswamy V, Daniels C, et al. **Review of molecular classification and treatment implications of pediatric brain tumors.** *Curr Opin Pediatr* 2018;30:3–9 CrossRef Medline
8. Jünger ST, Mynarek M, Wohlers I, et al. **Improved risk-stratification for posterior fossa ependymoma of childhood considering clinical, histological and genetic feature: a retrospective analysis of the HIT ependymoma trial cohort.** *Acta Neuropathol Commun* 2019;7:181 CrossRef Medline
9. Nowak J, Jünger ST, Huflage H, et al. **MRI phenotype of RELA-fused pediatric supratentorial ependymoma.** *Clin Neuroradiol* 2019;29:595–604 CrossRef Medline
10. Jaju A, Hwang EI, Kool M, et al. **MRI features of histologically diagnosed supratentorial primitive neuroectodermal tumors and pineoblastomas in correlation with molecular diagnoses and outcomes: a report from the Children's Oncology Group ACNS0332 trial.** *AJNR Am J Neuroradiol* 2019;40:1796–1803 Medline
11. Nowak J, Seidel C, Berg F, et al. **MRI characteristics of ependymoblastoma: results from 22 centrally reviewed cases.** *AJNR Am J Neuroradiol* 2014;35:1996–2001 CrossRef Medline
12. Stock A, Mynarek M, Pietsch T, et al. **Imaging characteristics of wingless pathway subgroup medulloblastomas: results from the German HIT/SIOP-trial cohort.** *AJNR Am J Neuroradiol* 2019;40:1811–17 CrossRef Medline
13. Nowak J, Nemes K, Hohm A, et al. **Magnetic resonance imaging surrogates of molecular subgroups in atypical teratoid/rhabdoid tumor.** *Neuro Oncol* 2018;20:1672–79 CrossRef Medline
14. Deng MY, Sill M, Sturm D, et al. **Diffuse glioneuronal tumour with oligodendroglioma-like features and nuclear clusters (DGONC): a molecularly defined glioneuronal CNS tumour class displaying recurrent monosomy 14.** *Neuropathol Appl Neurobiol* 2020;46:422–30 CrossRef Medline
15. Pickles JC, Mankad K, Aizpurua M, et al. **A case series of diffuse glioneuronal tumours with oligodendroglioma-like features and nuclear clusters (DGONC).** *Neuropathol Appl Neurobiol* 2020;47:464–67 CrossRef Medline
16. Holsten T, Lubieniecki F, Spohn M, et al. **Detailed clinical and histopathological description of 8 cases of molecularly defined CNS neuroblastomas.** *J Neuropathol Exp Neurol* 2021;80:52–59 CrossRef Medline